NIH Public Access
Author Manuscript
Mol Cell Neurosci. Author manuscript; available in PMC 2009 February 1.

Published in final edited form as:
Mol Cell Neurosci. 2008 February ; 37(2): 412–424.

Phosphodiesterase-Iα/Autotaxin's MORFO domain regulates oligodendroglial process network formation and focal adhesion organization

Jameel Dennis[1], **Michael A. White**[1], **Audrey D. Forrest**[1], **Larra M. Yuelling**[1], **Luciana Nogaroli**[1,2], **Fatemah S. Afshari**[1], **Michael A. Fox**[1], and **Babette Fuss**[1]

1 *Department of Anatomy and Neurobiology, Virginia Commonwealth University School of Medicine, Richmond, Virginia 23298, USA*

2 *Graduate Program in Biological Sciences, Institute of Biophysics Carlos Chagas Filho, Federal University of Rio de Janeiro, Rio de Janeiro, RJ 21941-590, Brazil*

Abstract

Development of a complex process network by maturing oligodendrocytes is a critical but currently poorly characterized step toward myelination. Here, we demonstrate that the matricellular oligodendrocyte-derived protein phosphodiesterase-Iα/autotaxin (PD-Iα/ATX) and especially its MORFO domain are able to promote this developmental step. In particular, the single EF hand-like motif located within PD-Iα/ATX's MORFO domain was found to stimulate the outgrowth of higher order branches but not process elongation. This motif was also observed to be critical for the stimulatory effect of PD-Iα/ATX's MORFO domain on the reorganization of focal adhesions located at the leading edge of oligodendroglial protrusions. Collectively, our data suggest that PD-Iα/ATX promotes oligodendroglial process network formation and expansion via the cooperative action of multiple functional sites located within the MORFO domain and more specifically, a novel signaling pathway mediated by the single EF hand-like motif and regulating the correlated events of process outgrowth and focal adhesion organization.

Introduction

Oligodendrocytes are the myelin producing cells of the central nervous system (CNS) that ensheath axonal segments and thereby allow saltatory conduction and efficient nerve signal propagation. During development, bipolar oligodendrocyte progenitor cells migrate from restricted sites of origin to appropriate target areas where they differentiate in a cell autonomous fashion into post-migratory, premyelinating oligodendrocytes. These maturing oligodendrocytes extend a highly complex process network to maximize sampling of the environment for axonal segments ready to be myelinated (Abney et al., 1981; Kachar et al., 1986; Knapp et al., 1987; Pfeiffer et al., 1993; Knapp, 1997; Buttery and ffrench-Constant, 2001; Miller, 2002; Fox et al., 2006; Kirby et al., 2006). Thus, the establishment of a complex and expanded oligodendroglial process network is critical for efficient myelination.

Corresponding author: Babette Fuss, Department of Anatomy and Neurobiology, Virginia Commonwealth University, PO Box 980709, Richmond, VA 23298, Phone: (804) 827 0926, Fax: (804) 828 9477, E-mail: bfuss@vcu.edu.

Publisher's Disclaimer: This is a PDF file of an unedited manuscript that has been accepted for publication. As a service to our customers we are providing this early version of the manuscript. The manuscript will undergo copyediting, typesetting, and review of the resulting proof before it is published in its final citable form. Please note that during the production process errors may be discovered which could affect the content, and all legal disclaimers that apply to the journal pertain.

NIH-PA Author Manuscript
NIH-PA Author Manuscript
NIH-PA Author Manuscript

NIH-PA Author Manuscript

NIH-PA Author Manuscript

NIH-PA Author Manuscript

Oligodendroglial process network formation, characterized by the generation and remodeling of higher order branches and interconnections, is initialized by well-coordinated changes in the organization of the actin cytoskeleton (Wilson and Brophy, 1989; Richter-Landsberg, 2000; Song et al., 2001; Liu et al., 2003; Jiang et al., 2005; Williams et al., 2005; Brockschnieder et al., 2006; Nielsen et al., 2006). In non-process bearing, migratory cells such actin cytoskeletal changes are to a large extent controlled by two interdependent mechanisms: 1) modifications of the extracellular environment and 2) the recruitment, retention and dissociation of molecules from focal adhesions, i.e. intracellular signaling complexes linking the extracellular environment at sites of integrin binding and clustering with the cell's actin cytoskeleton (Burridge et al., 1988; Jockusch et al., 1995; Zamir and Geiger, 2001; Martin et al., 2002; Zaidel-Bar et al., 2004). Integrin receptors have been implicated in the regulation of process outgrowth from post-migratory, premyelinating oligodendrocytes, and focal adhesion kinase has been found expressed in these cells (Buttery and ffrench-Constant, 1999; Kilpatrick et al., 2000; Cohen et al., 2003; Liang et al., 2004; Cohen, 2005; Olsen and ffrench-Constant, 2005). Furthermore, changes in the extracellular environment have been associated with an inhibition of oligodendroglial process outgrowth (Ricard et al., 2000; Ricard et al., 2001; Cohen et al., 2003; Cohen, 2005). However, the extracellular factors promoting morphological maturation of post-migratory, premyelinating oligodendrocytes and the role of focal adhesion organization in the distinct actions of oligodendroglial processes are largely unknown.

Our previous studies identified phosphodiesterase-Iα/autotaxin (PD-Iα/ATX), also designated pyrophosphatase/phosphodiesterase 2 (NPP2), as a protein that is released by post-migratory, premyelinating oligodendrocytes during the developmental stages of initial myelination (Fuss et al., 1997; Fox et al., 2003; see also Dugas et al., 2006; Nielsen et al., 2006; Savaskan et al., 2006). Functionally, PD-Iα/ATX possesses active adhesion-antagonizing, i.e. matricellular, properties toward differentiating post-migratory oligodendrocytes but not migratory oligodendrocyte progenitor cells (Fox et al., 2004). Thus, at a stage of oligodendrocyte development when process outgrowth is prominent, PD-Iα/ATX represents an extracellular factor that supports intermediate adhesive states known to be highly amenable to morphological remodeling (Murphy-Ullrich, 2001; Bornstein and Sage, 2002; Fox et al., 2004). PD-Iα/ATX has long been recognized to stimulate cell motility via its enzymatic, i.e. lysophospholipase D (lysoPLD), activity (Lee et al., 1996; Bollen et al., 2000; Clair et al., 2003; Gijsbers et al., 2003; Koh et al., 2003; Hama et al., 2004; Moolenaar et al., 2004; Xie and Meier, 2004). However, the above described effects on post-migratory oligodendrocytes have been observed in the absence of PD-Iα/ATX's lysoPLD-active site, and they were found to be mediated by the C-terminal region of PD-Iα/ATX, here referred to as the modulator of oligodendrocyte remodeling and focal adhesion organization (MORFO) domain (Fox et al., 2004; Dennis et al., 2005). Within the sequence of the MORFO domain one conserved structure-function motif has been identified, namely the EF hand-like motif. This motif is phylogenetically conserved (80% identity in the loop region between rat and human) and not required for the enzymatic activity of PD-Iα/ATX (Lee et al., 2001). EF hands are primarily known as calcium sensors (Lewit-Bentley and Rety, 2000). However, there is increasing evidence that they can perform additional and potentially calcium-binding-independent functions (Nelson and Chazin, 1998; Busch et al., 2000).

Here, we demonstrate that PD-Iα/ATX, as part of the extracellular environment and via its MORFO domain, not only supports a malleable cellular state but actively promotes the establishment of a complex and expanded oligodendroglial process network. This effect is associated with a reorganized assembly of focal adhesions located primarily at the leading edge of cellular protrusions, and it is, at least in part, mediated by the single EF hand-like motif located within PD-Iα/ATX's MORFO domain.

NIH-PA Author Manuscript
NIH-PA Author Manuscript
NIH-PA Author Manuscript

Results

PD-Iα/ATX promotes oligodendroglial process outgrowth via its MORFO domain

To explore the effects of PD-Iα/ATX's MORFO domain on morphological remodeling of oligodendroglial cells, we first analyzed cells of the oligodendroglial CIMO cell line (Bronstein et al., 1998). These cells represent an ideal tool for investigating cellular responses to exogenous PD-Iα/ATX since they respond to the adhesion-antagonizing activity of PD-Iα/ATX's MORFO domain to a similar extent as primary oligodendrocytes (Fig. 1A and Fox et al., 2004) but do not express endogenous PD-Iα/ATX (data not shown). When adhering to control substrates (rLacZ) CIMO cells extended broad and flat protrusions (Fig.1B; left panels). In contrast, on substrates containing full length r(recombinant)PD-Iα/ATX (not shown) or rPD-Iα/ATX-MORFO CIMO cells extended distinct processes and exhibited an elevated cell body (Fig. 1B; right panels). These findings provided the first evidence that PD-Iα/ATX's MORFO domain stimulates oligodendroglial process outgrowth.

To investigate process outgrowth in primary oligodendrocytes, oligodendrocyte progenitor cells were allowed to differentiate in the presence of rPD-Iα/ATX-MORFO or rControl and then labeled with the O4 antibody. Oligodendrocyte progenitor cells were chosen for initial plating since they are unresponsive to PD-Iα/ATX-MORFO's effect on cell adhesion and do not express PD-Iα/ATX endogenously (Fox et al., 2004). Once cells express the O4 surface antigen, they are considered post-migratory, premyelinating cells that are responsive to PD-Iα/ATX's MORFO domain (Warrington et al., 1992; Pfeiffer et al., 1993; Fox et al., 2004). However, O4-positive cells begin to release endogenous PD-Iα/ATX (Fox et al., 2003), thus limiting the timeframe during which significant differences upon addition of exogenous PD-Iα/ATX can be observed. Therefore, cells were analyzed 48 hrs after plating. Due to the complexity of the process network established by post-migratory, premyelinating oligodendrocytes we defined as a quantitative measurement for process outgrowth and network formation a process and complexity index, respectively. The process index represents the total amount of O4-positive process surfaces per cell, while the complexity index reflects a ratio of process index to total area occupied by the cell's process network (for details see process morphology assay in the experimental methods section). At the time-point of analysis membranous structures were rare or absent, thus largely restricting our analysis to the morphology of fine processes. When plotting the process indices of all cells against their complexity indices a scattered distribution was observed (Fig. 2A). In the presence of rPD-Iα/ATX-MORFO this scattered distribution shifted toward the upper right quadrant. This shift reflects a significant increase in the percentage of cells that are characterized by both process and complexity indices larger than the mean value determined for cells plated on rControl-containing substrates (Fig. 2A and B). In addition, application of rPD-Iα/ATX-MORFO resulted in cells with larger process (>150) and complexity (>252) indices than seen for any of the cells under control conditions.

To further substantiate the stimulatory role of PD-Iα/ATX on oligodendroglial process network formation, differentiating post-migratory oligodendrocytes were treated with a siRNA pool specific to PD-Iα/ATX (siPD-Iα/ATX) 48 hrs after plating. Cells were analyzed 48 hrs subsequent to siRNA application, i.e. 96 hrs after plating. At this time-point, PD-Iα/ATX mRNA and protein levels were reduced by at least 50% (see supplementary Fig. 1). Under these conditions and compared to control conditions the oligodendroglial process network was characterized by smaller process and complexity indices (Fig. 2C and D). As indicated above, the siRNA-treated cells were more mature than those analyzed in the studies presented in Fig. 2A and B. Thus, few cells had begun to develop membranous structures. In the scatter plots and bar graphs presented, cells with extensive myelin membrane-like structures were excluded. In addition, while a decrease in membranous structures would lead to a decrease in process index, such a decrease would not contribute to the observed decrease in the complexity index

NIH-PA Author Manuscript

NIH-PA Author Manuscript

NIH-PA Author Manuscript

since membranous structures are characterized by a complexity index of 0. Thus, our data demonstrate that PD-Iα/ATX plays an important and stimulatory role for the formation of the complex actin filament-rich process network that is established by post-migratory, premyelinating oligodendrocytes at both the early and later developmental stages analyzed here. Furthermore, it does so as an extracellular factor and via its MORFO domain.

PD-Iα/ATX's MORFO domain mediates an increase in oligodendroglial process network formation in part via its EF hand-like motif

To further define the functional site responsible for the stimulatory effect of PD-Iα/ATX's MORFO domain on oligodendroglial process network formation, we focused on the only known structure-function motif located within this area of the protein, the EF hand-like motif. First, a cyclic peptide was generated that represented the EF hand loop region plus neighboring amino acids (EF peptide; see Fig. 3A). In the presence of this EF peptide oligodendrocytes established a highly branched process network (Fig. 3D). However, this process network appeared condensed compared to the one established in the presence of the MORFO domain (compare upper left panel of Fig. 3D with upper left panel of Fig. 3E). Indeed, when determining the area covered by the oligodendroglial process network (network area=white area in insets to Fig. 3E, upper panel), no increase over control was noted for the EF peptide (Fig. 3B). In contrast, this area was significantly enlarged in the presence of rPD-Iα/ATX-MORFO (Fig. 3B) due to an increase in both process and complexity indices (Fig. 3C). In the case of the EF peptide our morphology analysis revealed no significant changes in either of the two indices, despite the apparent difference in complexity upon visual inspection of the cells' morphology (Fig. 3D). This observation does not reflect a discrepancy but rather reveals that the complexity of a very dense process network, as seen in the presence of the EF peptide, is difficult to resolve, and that the EF peptide alone does not lead to a significant increase in process index. Thus, our data suggest that the EF hand-like motif promotes the outgrowth of higher order processes at the expense of process elongation and network expansion. They further suggest that PD-Iα/ATX's MORFO domain may possess an EF hand-like motif-independent ability to promote process elongation and network expansion.

Highly conserved aspartic acid residues (D) at positions 1, 5 and 9 of EF hand loop regions have been shown to significantly contribute to the functional properties of EF hand proteins (Babu et al., 1992; Prod'hom and Karplus, 1993; Drake et al., 1996). For PD-Iα/ATX, substitution of these aspartic acid residues with asparagine residues (N) (Fig. 3A, EF D→N peptide) eliminated to some extent the effect of the EF peptide on the compactness and complexity of the oligodendroglial process network (Fig. 3D). In fact, the process network area was found to be slightly increased, i.e. less compacted, when compared to the one established in the presence of the EF or control peptide (Figs. 3B and D). Similarly, introduction of the D to N mutation into rPD-Iα/ATX-MORFO (rPD-Iα/ATX-MORFO D→N) yielded an increase in process network area when compared to rPD-Iα/ATX-MORFO or control protein (Fig. 3B and E). This increase in area was found to be due to an increase in process index for the EF D→N peptide and in both process and complexity indices for the rPD-Iα/ATX-MORFO D→N protein (Fig. 3C). Taken together, the above findings demonstrate an important role for the aspartic acid residues (positions 1, 5 and 9) of PD-Iα/ATX's EF hand loop region for the regulation of oligodendroglial process network formation and expansion.

Interestingly, deletion of the EF hand-like motif (rPD-Iα/ATX-MORFO ΔEF) eliminated the stimulatory effect of rPD-Iα/ATX-MORFO on both process outgrowth and elongation (Fig. 3B, C and E). This outcome is likely due to a conformational change leading to a reduction in overall PD-Iα/ATX-MORFO function; an interpretation that is supported by a reduction in secretion and enzymatic activity of a similarly mutated full length PD-Iα/ATX protein expressed by eukaryotic cells (our unpublished observations and Lee et al., 2001). Thus, the

NIH-PA Author Manuscript

NIH-PA Author Manuscript

NIH-PA Author Manuscript

above data demonstrate that PD-Iα/ATX's EF hand-like motif plays a crucial role in regulating the outgrowth of in particular higher order oligodendroglial processes, and they suggest that process elongation and network expansion may be stimulated by an additional yet to be characterized functionally active site within PD-Iα/ATX's MORFO domain.

PD-Iα/ATX's MORFO domain attenuates the association of paxillin with focal adhesions in oligodendroglial cells via its EF hand-like motif

The above described effects of extracellular rPD-Iα/ATX-MORFO on actin filament-rich oligodendroglial processes and the importance of focal adhesions for tethering the actin cytoskeleton to the extracellular matrix (ECM) suggest changes in focal adhesion organization to be one of the primary targets of PD-Iα/ATX's MORFO domain. We first focused on the focal adhesion adaptor protein paxillin since it is well known for its central role in integrating signals from the extracellular environment to affect cellular remodeling (Brown and Turner, 2004). Paxillin-containing focal adhesions were located primarily at the leading edge of protrusions in CIMO cells cultured on control substrates (Fig. 4A). Similarly, paxillin-containing complexes in the size of small focal adhesions could be detected at the tips of oligodendroglial processes, i.e. in OLG-growth cones (Fig. 4B; Fox et al., 2006). Our previous data using the oligodendroglial cell line N19 demonstrated that PD-Iα/ATX's MORFO domain increases the distribution of paxillin to the detergent soluble fraction in oligodendroglial cells (Fox et al., 2004). In agreement with these findings is our observation that the number of paxillin-containing focal adhesions was significantly reduced in the presence of rPD-Iα/ATX-MORFO in CIMO cells (Fig. 4C and D). Thus, PD-Iα/ATX's MORFO domain attenuates the association of paxillin with focal adhesions and the detergent-insoluble cytoskeleton in oligodendroglial cells.

To assess the extent to which PD-Iα/ATX's enzymatically active site may influence this MORFO-domain mediated effect on paxillin distribution, we performed focal adhesion assays using native full length rPD-Iα/ATX and an enzymatically inactive mutant form of the protein (rPD-Iα/ATX-T210A; see Clair et al., 1997; Gijsbers et al., 2003; Koh et al., 2003). As expected, only the native form of PD-Iα/ATX was able to function as lysoPLD (Fig. 4E). In focal adhesion assays both protein forms affected the number of paxillin-containing focal adhesions to the same extent (Fig. 4F). These data demonstrate that PD-Iα/ATX's effect on paxillin is 1) mediated by its MORFO domain and 2) independent of its lysoPLD active site.

Given the above established critical role of the EF hand-like motif for MORFO domain-stimulated process outgrowth, we assessed the extent to which this motif may be involved in regulating the distribution of paxillin. Deletion of the EF hand loop region eliminated the effect of rPD-Iα/ATX-MORFO on paxillin-containing focal adhesions (Fig. 5A). Furthermore, the EF peptide alone was able to fully mimic the effect of rPD-Iα/ATX-MORFO on the number of paxillin-containing focal adhesions, indicating that the EF hand-like motif is necessary and may be sufficient for promoting the observed redistributed localization of paxillin. Mutation of the aspartic acid residues at positions 1, 5 and 9 of the EF hand loop region abolished the ability of both rPD-Iα/ATX-MORFO and the EF peptide to reduce the number of paxillin-containing focal adhesions. Instead, this mutation caused an increase in recruitment of paxillin to focal adhesions. Taken together, the above data demonstrate that the EF hand-like motif is not only crucial for promoting the outgrowth of in particular higher order processes but also for stimulating the redistribution of paxillin away from focal adhesions and the cytoskeleton. In addition and as for the regulation of oligodendroglial process outgrowth, the aspartic acid residues at positions 1, 5 and 9 of the EF hand loop region appear to play an important role for regulating the distribution of paxillin.

NIH-PA Author Manuscript

NIH-PA Author Manuscript

NIH-PA Author Manuscript

PD-Iα/ATX's MORFO domain affects the molecular composition of focal adhesions

Changes in the molecular composition of focal adhesions and thus the efficiency of the linkage between the ECM and the actin cytokeleton are known to be associated with cellular remodeling (Zamir and Geiger, 2001; Brown et al., 2006). In our earlier studies using cells of the N19 cell line, we not only observed increased levels of detergent-soluble paxillin in the presence of rPD-Iα/ATX-MORFO; we also found increased detergent-soluble levels of the actin-binding focal adhesion component vinculin in response to rPD-Iα/ATX-MORFO (Fox et al., 2004). However, this effect was significantly less prominent than the one seen for paxillin (46% and 110% for vinculin and paxillin, respectively). Determining the number of vinculin-containing focal adhesions in CIMO cells without prior detergent treatment and in the presence of native and mutated rPD-Iα/ATX-MORFO protein as well as native and mutated EF peptide revealed no significant changes (Fig. 5B). Thus, as in our earlier studies PD-Iα/ATX's MORFO domain exerted a significantly more pronounced change in distribution for the focal adhesion component paxillin compared to vinculin. We, therefore, conclude from these data that vinculin appears to remain in complex with other focal adhesion proteins located at the cell surface. However, the strength with which this complex is associated with the actin cytoskeleton is weakened, thus leading to an increase in detergent solubility. In support of this interpretation is the observation that for both vinculin and paxillin the levels of increase in the detergent-soluble fraction are considerably greater than the levels of decrease in paxillin-containing focal adhesions in untreated cells (46% vs. undetectable for vinculin and 210% vs. 40% for paxillin). Furthermore, in preliminary studies we found that the detergent-soluble levels of vinculin are increased in the presence of rPD-Iα/ATX-MORFO (data not shown). Taken together, the above findings indicate that upon interaction of PD-Iα/ATX's MORFO domain with the oligodendroglial cell surface the link between the ECM and the actin cytoskeleton may be weakened at a point close to the actin cytoskeleton (see model in Fig. 6). To further substantiate this idea, we assessed the effect of PD-Iα/ATX's MORFO domain on focal adhesions containing α-actinin, an actin-binding focal adhesion component previously shown to be dispersed upon weakening of the ECM-cytoskeletal linkage (Laukaitits et al., 2001). As expected, the number of α-actinin-containing focal adhesions was significantly reduced in response to PD-Iα/ATX's MORFO domain (Fig. 5C).

Discussion

During central nervous system development post-migratory, premyelinating oligodendrocytes undergo extensive morphological remodeling. In particular, they establish a large and highly branched process network to efficiently sample their environment for axonal segments ready to be myelinated. The studies presented here identify PD-Iα/ATX, a protein released by differentiating oligodendrocytes, as a novel extracellular factor promoting outgrowth and expansion of the oligodendroglial process network. This effect is mediated by PD-Iα/ATX's MORFO domain and seems accompanied by the dispersal of in particular paxillin- and α-actinin from focal adhesions located at the leading edge of cellular protrusions. The structure-function motif primarily responsible for the MORFO domain-mediated changes in focal adhesion organization appears to be the EF hand-like motif. This motif also promotes the outgrowth of in particular higher order processes, however, at the expense of process elongation. Based on the above data, we propose a model (Fig. 6), in which PD-Iα/ATX's MORFO domain stimulates the redistribution of paxillin and α-actinin at least in part via its EF hand-like motif. It thereby weakens the cytoskeleton-ECM link and promotes oligodendroglial process outgrowth. Process elongation and network expansion, on the other hand, appear to be stimulated by an additional yet uncharacterized functionally active site located within PD-Iα/ATX's MORFO domain.

NIH-PA Author Manuscript

NIH-PA Author Manuscript

NIH-PA Author Manuscript

Our data demonstrate a stimulatory role of PD-Iα/ATX and in particular its MORFO domain on oligodendroglial process network formation. This effect appears restricted to post-migratory, premyelinating stages of the oligodendrocyte lineage. Therefore, a subpopulation of cells remained unaffected in our assays using enriched oligodendroglial cultures (see Fig. 2A). These cultures are unsynchronized with regard to their developmental stage and include yet undifferentiated oligodendrocyte progenitor cells and/or developmentally quiescent cells potentially representing a correlate to the adult progenitor cell (Gard and Pfeiffer, 1989;Hardy and Reynolds, 1991).

Process network formation and expansion is a morphological hallmark of oligodendrocyte maturation. During normal development it is associated with an increased expression of myelin proteins, such as myelin basic protein (MBP) (Zeller et al., 1985; Dubois-Dalcq et al., 1986; Hardy and Friedrich, 1996). Under experimental conditions, morphological maturation of oligodendrocytes can occur in the absence of an increase in myelin gene expression, suggesting that these two events may be regulated independently from each other (Buttery and ffrench-Constant, 1999; Osterhout et al., 1999; Sloane and Vartanian, 2007). In the case of PD-Iα/ATX's MORFO domain we currently favor a model in which primarily morphological remodeling is affected. However, at this point we cannot exclude concomitant changes in the expression of myelin proteins.

Based on our data morphological maturation of the oligodendroglial process network is likely dependent on a well-coordinated regulation of focal adhesion organization. The previous observation that patches of high levels of phosphotyrosine are not associated with areas of substrate attachment in differentiating oligodendrocytes is not necessarily in disagreement with the above stated importance of focal adhesions (Ranjan and Hudson, 1996; Buttery and ffrench-Constant, 2001). First, differentiation of oligodendrocytes is associated with a decrease rather than increase in phosphorylation of at least the tyrosine 925 site of focal adhesion kinase (Fig. 6 and Fox et al., 2004). Thus, focal adhesion signaling complexes may be of relatively low phosphotyrosine content compared to other signaling complexes, such as those assembled in lipid rafts. Furthermore, efficient process remodeling requires not only the formation of focal adhesions but also their turnover and disassembly (Webb et al., 2002). In agreement with this concept is our finding that PD-Iα/ATX's MORFO domain promotes not only process remodeling but also a reduction in the number of paxillin- and α-actinin-containing focal adhesions. Indeed, small focal adhesions of high turnover/disassembly and weak binding strength to the actin cytoskeleton are thought to be a typical feature of a cell undergoing highly dynamic remodeling (Laukaitis et al., 2001; Brown et al., 2006; Zaidel-Bar et al., 2007). In contrast to paxillin- and α-actinin, vinculin-containing complexes can remain at the cell surface after weakening of the ECM-cytoskeleton link. They are then recycled by translocation or 'sliding' (Laukaitis et al., 2001; Webb et al., 2002). Our data suggest a similar mechanism for vinculin in response to PD-Iα/ATX's MORFO domain. So far, immortalized oligodendroglial cell line responses to PD-Iα/ATX have been found comparable to those observed in post-migratory, premyelinating oligodendrocytes (see for example Fig. 1; Fox et al., 2004). We thus consider it likely that with regard to focal adhesion organization the same mechanisms are operative in primary cells. However, at this point we cannot exclude subtle differences between the immortalized and the primary cells. Interestingly, changes in focal adhesion composition, similar to the ones observed here, have also been described for other extracellular proteins with adhesion-antagonizing, i.e. matricellular, properties (Miao et al., 2000; Peters et al., 2005). The matricellular proteins SPARC and thrombospondin have been shown to affect paxillin and vinculin equally, thus suggesting potential differences in molecular mechanisms despite an overall similar functional outcome (Murphy-Ullrich et al., 1993; Murphy-Ullrich et al., 1995; Murphy-Ullrich, 2001).

NIH-PA Author Manuscript

NIH-PA Author Manuscript

NIH-PA Author Manuscript

One of the structure-function motifs shown here to be critically involved in the regulation of oligodendroglial process outgrowth by PD-Iα/ATX's MORFO domain is the EF hand-like motif. There is only a single motif present in PD-Iα/ATX's MORFO domain. Thus, PD-Iα/ATX's EF hand-like motif is unlikely to function as a calcium sensor that generally requires EF hands to occur in pairs (Lewit-Bentley and Rety, 2000). Indeed, our data demonstrate that PD-Iα/ATX's EF hand-like motif possesses functional properties of its own (see Figs. 3 and 5). The existence of such an independent function of a single EF hand-like motif is further supported by the finding that one of the EF hand motifs of SPARC has been shown to confer adhesion-antagonizing properties (Murphy-Ullrich et al., 1995). However, as discussed above, different mechanisms seem to be initialized by these two similar motifs.

PD-Iα/ATX has been characterized as one of the major enzymes responsible for the extracellular generation of the lipid signaling molecule lysophosphatidic acid (LPA) (Tanaka et al., 2006; van Meeteren et al., 2006). Cell surface receptors known to mediate LPA signaling are expressed by post-migratory, premyelinating oligodendrocytes (Weiner et al., 1998; Stankoff et al., 2002; Yu et al., 2004). Thus, PD-Iα/ATX's enzymatic activity likely contributes to oligodendrocyte development and/or function. So far, however, the exact role of LPA signaling for post-migratory, premyelinating oligodendrocytes remains elusive. Our data demonstrate that PD-Iα/ATX has the ability to promote morphological maturation and focal adhesion reorganization in the absence of its lysoPLD activity. Furthermore, focal adhesion reorganization is not influenced by the LPA generating enzymatic activity of PD-Iα/ATX. Thus, it appears that it is primarily PD-Iα/ATX's MORFO domain that affects the morphological maturation of the fine process network of differentiating oligodendrocytes. However, future studies will be necessary to determine the exact contribution of each of PD-Iα/ATX's functionally active sites for the developmental progression and functional properties of cells of the oligodendrocyte lineage.

Experimental methods

Antibodies

Hybridoma clone A2B5 (ATCC, Manassas, VA) was used for immunopanning of oligodendrocyte progenitor cells. Hybridoma clone O4 (gift from S.E. Pfeiffer) was used to identify post-migratory, premyelinating oligodendrocytes (Sommer and Schachner, 1981; Bansal et al., 1989). Anti-vinculin, anti-paxillin (Millipore/Chemicon, Temecula, CA) and anti-α-actinin (Santa Cruz Biotechnologies, Santa Cruz, CA) antibodies were used for the focal adhesion analysis. For all immunostainings, Alexa 488-conjugated antibodies (Invitrogen/Molecular Probes, Carlsbad, CA) were used as secondary antibodies. Anti-Glutathione-S-transferase antibodies (BD Biosciences, San Jose, CA) in combination with horseradish peroxidase (HRP)-labeled secondary antibodies (Vector Laboratories, Burlingame, CA) were used for Western blots. Polyclonal anti-PD-Iα/ATX antibodies used for the analysis of cell culture supernatants were either generated by us (Fox et al., 2003) or kindly provided by T. Clair.

Animals

Sprague Dawley female rats with early postnatal litters were obtained from Zivic Miller (Pittsburg, PA). All animal studies were approved by the Institutional Animal Care and Use Committee at Virginia Commonwealth University.

Recombinant proteins and peptides

Histidine (His)-tagged fusion proteins were generated as described previously (Fox et al., 2003; Fox et al., 2004). Glutathione-S-transferase (GST)-tagged fusion proteins were generated in pGEX-KG using a cDNA clone encoding amino acids I^{390}-I^{885} of PD-Iα/ATX

NIH-PA Author Manuscript

NIH-PA Author Manuscript

NIH-PA Author Manuscript

(Guan and Dixon, 1991; Fuss et al., 1997). References to amino acid positions are according to the sequence published by Narita et al. (1994). No functional differences were observed between GST- and His-tagged PD-Iα/ATX-MORFO recombinant fusion proteins. As controls, His-tagged β-galactosidase (rLacZ) or a clone in which the PD-Iα/ATX MORFO domain had been inserted in the reverse orientation (rControl) were used for His- and GST-tagged proteins, respectively. rControl consists of primarily GST due to a stop codon at nucleotides 59–61 of the inverted insert sequence. No adverse effects have been observed when using either of the controls in any of the assays employed in the present study. MORFO ΔEF (ΔD^{762}-D^{773}), and MORFO D→ N (D762N, D766N, D770N) mutants were generated using the QuikChange II XL Site-Directed Mutagenesis Kit (Stratagene, La Jolla, CA). Sequence accuracy was confirmed by DNA sequencing.

Plasmids encoding the GST-tagged fusion proteins were transformed into competent BL-21 (DE3) codon plus cells (Invitrogen, Carlsbad, CA). After induction of protein expression, bacteria were grown for 18 hrs. Bacteria were resuspended in lysis buffer (20 mM Tris-HCl (pH 7.4), 300 mM NaCl, 1 mg/ml lysozyme, 5 mM Dithiothreitol, 1 μg/ml leupeptin, 1 μg/ml pepstatin) and sonicated. Bacterial cell debris was removed by centrifugation, supernatants were dialyzed overnight in 20 mM Tris-HCl (pH 7.4), passed through an ion exchange column and incubated overnight at 4 °C with glutathione conjugated sepharose beads (GE Healthcare BioSciences Corp., Piscataway, NJ). Fusion proteins were eluted in 50 mM Tris-HCl (pH 8.0)/ 4 mM Glutathione/30 mM NaCl, dialyzed against phosphate buffered saline (PBS) and quantified (BCA protein assay; Pierce, Rockford, IL). Proteins were analyzed by gel electrophoresis (Coomassie stain) along with Western blots.

Full length recombinant (r)PD-Iα/ATX fusion proteins were purified from Cos-7 cells stably transfected with a mammalian expression construct encoding rat PD-Iα/ATX including two carboxy-terminal tags (V5 and histidine (His); pEF/V5-His; Invitrogen, Carlsbad, CA). The single amino acid mutation (T210A), known to eliminate PD-Iα/ATX's enzymatic activity (Clair et al., 1997; Gijsbers et al., 2003; Koh et al., 2003), was introduced using the QuikChange II XL Site-Directed Mutagenesis Kit (Stratagene, La Jollla, CA). Full length rPD-Iα/ATX proteins (native and mutant) were secreted into the cell culture supernatant from where they were purified using the TALON Polyhistidine-Tag Purification Resin according to the manufacturer's instructions (Clontech, Mountain View, CA). As control, proteins unspecifically binding to the resin and "purified" from untransfected Cos-7 cell culture supernatants were used.

Cyclic peptides containing cysteine residues at either end to ensure native-like conformation (Le Clainche et al., 2003) and representing the loop region of PD-Iα/ATX's EF hand-like motif (EF peptide: CSGPIFDYNYDGLRDTEDEIKC), the loop region containing the MORFO D→N mutation (EF D→N peptide: CSGPIFNYNYNGLRNTEDEIKC) and a scrambled control (ctrl peptide: CESDEGNGDYDIKPIFYLRDTC) were custom synthesized (GenScript Corporation, Piscataway, NJ).

Cell culture

Primary rat oligodendrocyte progenitor cells were isolated from postnatal (day 3 or 4) rat brains as described previously (Barres et al., 1992; Fox et al., 2003). Briefly, cerebral hemispheres were minced and incubated in Hanks balanced salt solution supplemented with 0.25% trypsin (Invitrogen, Carlsbad, CA), and 1 μg/ml DNase (Sigma, St Louis, MO). After trituration, single cells were collected by centrifugation, resuspended in Dulbecco's Modified Eagle Medium (DMEM)/10% FCS (Invitrogen, Carlsbad, CA) and subjected to A2B5 (postnatal day 3) or O4 (postnatal day 4) immunopanning. Immunopanned cells were cultured in serum-free defined medium (DMEM containing 40 ng/ml tri-iodo-thyronine (T3; Sigma, St Louis, MO) and 1x N2 supplement (Invitrogen, Carlsbad, CA); DMEM/T3/N2) under the conditions indicated.

NIH-PA Author Manuscript

NIH-PA Author Manuscript

NIH-PA Author Manuscript

Cells of the immortalized mouse oligodendroglial cell line CIMO were cultured in DMEM/5% FCS/1 μg/ml interferon-γ (Millipore/Chemicon, Temecula, CA) at 33 °C (Bronstein et al., 1998).

Adhesion assay

Adhesion assays were performed as described previously (Fox et al., 2003; Fox et al., 2004).

Scanning electron microscopy

CIMO cells were plated on glass coverslips coated with fibronectin (10 μg/ml) and recombinant fusion protein (50 μg/ml) or synthetic peptide (200 μg/ml) and cultured for 1 hr in serum-free defined medium (DMEM/T3/N2) at 33 °C and 5% CO_2. Subsequently, cells were fixed and treated for scanning electron microscopy as described previously (Fox et al., 2006).

Process morphology assay

A2B5-immunopanned (see cell culture) or siRNA-treated (see siRNA-mediated knock-down) cells were plated onto glass coverslips. In the case of A2B5-immunopanned cells, coverslips were pre-coated with tagged fusion proteins (50 μg/ml) or synthetic peptides (200 μg/ml) in mixture with fibronectin (10 μg/ml). Significant effects were observed at these substrate concentrations in adhesion and focal adhesion assays (Fox et al., 2003 and data not shown). Considerable differences in coating efficiencies between the native and mutant forms of the fusion proteins were not observed (data not shown) and are considered unlikely for the peptides due to the nature of the mutations. In addition, the peptide concentrations used in these studies are comparable to those utilized in similar studies investigating matricellular protein function (Murphy-Ullrich et al., 1995).

After plating, cells were cultured in serum-free defined medium (DMEM/T3/N2) for 24 hrs. Subsequently, the cell culture medium was replaced with medium containing the fusion protein or synthetic peptide used for coverslip coating. After an additional 24 hrs, cells were fixed, washed and immunostained with O4 antibodies. Images of approximately 30 cells were taken randomly for each treatment group in each experiment ($n \geq 4$) using an Olympus BX51 inverted fluorescent microscope (Olympus America Inc., Center Valley, PA). IP Lab imaging software (BD Biosciences Bioimaging, Rockville, MD) was used to determine process index (total area found to be O4-positive after staining minus the cell body), network area (total area within the radius of process network surrounding the cell body minus the cell body) and complexity index (1 - process index/network area). To obtain scatter plots, mean values for process and complexity indices were calculated for each experiment for cells cultured on rControl protein. These mean values were set to 50 and adjusted, i.e. normalized, values for all cells were plotted on logarithmic scales. For the bar graphs representing network areas, the mean network area value for cells cultured on rControl protein was calculated. This mean value was set to 100% and adjusted, i.e. normalized, values for all cells were averaged for each experimental condition. To obtain 2D graphs depicting process and complexity indices, the mean values for cells cultured on rControl protein were calculated. These mean values were set to 100% and adjusted, i.e. normalized, values for all cells were averaged for each experimental condition.

si-RNA-mediated knock-down of PD-Iα/ATX expression in post-migratory, premyelinating oligodendrocytes

Post-migratory, premyelinating oligodendrocytes were isolated by O4-immunopanning from postnatal day 4 rat brains and plated onto fibronectin (10μg/ml)-coated glass coverslips. Cells were cultured in serum-free defined medium for 2 days. Subsequently, cells were transfected with siRNA (100 nM) using lipofectamine 2000 (Invitrogen, Carlsbad, CA) according to the manufacturer's instructions. SMARTpool siRNA directed against rat PD-Iα/ATX and control

NIH-PA Author Manuscript

NIH-PA Author Manuscript

NIH-PA Author Manuscript

non-targeting SMARTpool siRNA were obtained from Dharmacon Inc. (Lafayette, CO). Transfection medium containing siRNA-lipofectamine complexes was replaced with serum-free defined medium (DMEM/T3/N2) after 3 hrs and cells were cultured for an additional 48 hrs. Knock-down of PD-Iα/ATX was assessed by quantitative real-time RT PCR and by Western blot analysis of cell culture supernatants (see supplementary Fig 1).

PD-Iα/ATX-lysoPLD Activity Assay

PD-Iα/ATX's lysoPLD activity was determined using the fluorogenic assay described by Ferguson et al. (2006). Briefly, purified recombinant proteins (1 μg/ml) were incubated with 2.5 μM FS-3 substrate (Echelon Biosciences Inc., Salt Lake City, UT) in 140 mM NaCl, 5 mM KCl, 1 mM $CaCl_2$, 1 mM $MgCl_2$, 5 mM Tris/HCl (pH 8.0), 1 mg/ml fatty-acid-free BSA (Sigma-Aldrich, St. Louis, MO) for 8 hrs at 37 °C. Fluorescence intensities were measured at an excitation wavelength of 485nm and an emission wavelength of 520 nm using a FLUOstar multimode microplate reader (BMG LABTECH Inc. Durham, NC).

Focal Adhesion Analysis

Glass coverslips were coated with mixed substrates as described previously (Fox et al., 2004). Briefly, 2×10^3 CIMO cells were plated onto coverslips and allowed to attach for 1 hr. Cells were fixed in 4% paraformaldehyde and then permeabilized with 1% Triton X-100. After incubation in blocking solution (DMEM, 10% FCS), cells were incubated with anti-paxillin (1:100), anti-vinculin (1:100) or anti-α-actinin (1:100) antibodies over night at 4 °C. Bound primary antibodies were visualized using Alexa 488-conjugated secondary antibodies (1:250). Cells were analyzed using a confocal laser scanning microscope (TCS SP2 AOBS, Leica Microsystems, Exton, PA or LSM 510 META, Carl Zeiss MicroImaging, Inc., Thornwood, NY). For analysis of focal adhesions, images of the basal substrate-contacting surfaces of randomly selected cells were taken (Z depth: ~ 250nm). The number of focal adhesions, i.e. complexes of approximately 1 μm^2 and larger in size (Balaban et al., 2001), were determined by "particle counting" using the ImageJ software package (Abramoff et al., 2004).

Nucleofection of primary oligodendrocytes

A2B5-positive oligodendrocytes were isolated from postnatal day 3 rat pups (see cell culture) and incubated in suspension in DMEM/10% FCS for 1.5 hrs at 37 °C and 5% CO_2. Cells were collected by centrifugation (1000 rpm for 5min) and nucleofected with 0.5μg Paxillin-EGFP encoding plasmid DNA (kindly provided by Rick Horwitz) using the rat oligodendrocyte nucleofection kit according to the manufacturer's instructions (amaxa Inc., Gaithersburg, MD). Cells were resuspended in serum-free defined medium (DMEM/T3/N2) and plated onto Lab-Tek II glass chamber slides (Nalge Nunc International, Naperville, IL) pre-coated with fibronectin (10μg/ml). Cells were maintained at 37 °C, 5% CO_2 for 24 hrs. Paxillin-EGFP-positive oligodendrocytes of post-migratory morphology were visualized using a confocal microscope (Zeiss LSM 510 META NLO; Carl Zeiss MicroImaging, Inc., Thornwood, NY).

Supplementary Material

Refer to Web version on PubMed Central for supplementary material.

Acknowledgements

The authors thank J. Bronstein for the oligodendroglial CIMO cell line, S. Pfeiffer for the hybridoma cell line O4, R. Horwitz for the plasmid encoding Paxillin-EGFP and T. Clair for polyclonal anti-PD-Iα/ATX antibodies. Confocal, fluorescent, and scanning electron microscopy was performed at VCU's Department of Neurobiology and Anatomy Microscopy Facility with assistance from J. Williamson and S. Henderson; plasmid cloning procedures were performed with assistance of K. Gorse at VCU's Department of Neurobiology and Anatomy Molecular Biology Facility. Both facilities were supported, in part, through NIH-NINDS Center core grant 5P30NS047463. This work was supported

NIH-PA Author Manuscript

NIH-PA Author Manuscript

NIH-PA Author Manuscript

by grants from the National Institute of Health (B.F), the National Multiple Sclerosis Society (B.F.) and a Predoctoral Kirschstein-NRSA (M.A.F.).

References

Abney ER, Bartlett PP, Raff MC. Astrocytes, ependymal cells, and oligodendrocytes develop on schedule in dissociated cell cultures of embryonic rat brain. Dev Biol 1981;83:301–310. [PubMed: 7239014]

Abramoff MD, Magelhaes PJ, Ram SJ. Image Processing with ImageJ. Biophotonics International 2004;11:36–42.

Babu A, Su H, Ryu Y, Gulati J. Determination of residue specificity in the EF-hand of troponin C for Ca2+ coordination, by genetic engineering. J Biol Chem 1992;267:15469–15474. [PubMed: 1639788]

Balaban NQ, Schwarz US, Riveline D, Goichberg P, Tzur G, Sabanay I, Mahalu D, Safran S, Bershadsky A, Addadi L, Geiger B. Force and focal adhesion assembly: a close relationship studied using elastic micropatterned substrates. Nat Cell Biol 2001;3:466–472. [PubMed: 11331874]

Bansal R, Warrington AE, Gard AL, Ranscht B, Pfeiffer SE. Multiple and novel specificities of monoclonal antibodies O1, O4, and R-mAb used in the analysis of oligodendrocyte development. J Neurosci Res 1989;24:548–557. [PubMed: 2600978]

Barres BA, Hart IK, Coles HS, Burne JF, Voyvodic JT, Richardson WD, Raff MC. Cell death and control of cell survival in the oligodendrocyte lineage. Cell 1992;70:31–46. [PubMed: 1623522]

Bollen M, Gijsbers R, Ceulemans H, Stalmans W, Stefan C. Nucleotide pyrophosphatases/phosphodiesterases on the move. Crit Rev Biochem Mol Biol 2000;35:393–432. [PubMed: 11202013]

Bornstein P, Sage EH. Matricellular proteins: extracellular modulators of cell function. Curr Opin Cell Biol 2002;14:608–616. [PubMed: 12231357]

Brown MC, Turner CE. Paxillin: adapting to change. Physiol Rev 2004;84:1315–1339. [PubMed: 15383653]

Brown CM, Hebert B, Kolin DL, Zareno J, Whitmore L, Horwitz AR, Wiseman PW. Probing the integrin-actin linkage using high-resolution protein velocity mapping. J Cell Sci 2006;119:5204–5214. [PubMed: 17158922]

Brockschnieder D, Sabanay H, Riethmacher D, Peles E. Ermin, a myelinating oligodendrocyte-specific protein that regulates cell morphology. J Neurosci 2006;26:757–762. [PubMed: 16421295]

Bronstein JM, Hales TG, Tyndale RF, Charles AC. A conditionally immortalized glial cell line that expresses mature myelin proteins and functional GABA(A) receptors. J Neurochem 1998;70:483–491. [PubMed: 9453541]

Burridge K, Fath K, Kelly T, Nuckolls G, Turner C. Focal adhesions: transmembrane junctions between the extracellular matrix and the cytoskeleton. Annu Rev Cell Biol 1988;4:487–525. [PubMed: 3058164]

Busch E, Hohenester E, Timpl R, Paulsson M, Maurer P. Calcium affinity, cooperativity, and domain interactions of extracellular EF-hands present in BM-40. J Biol Chem 2000;275:25508–25515. [PubMed: 10801822]

Buttery PC, ffrench-Constant C. Laminin-2/integrin interactions enhance myelin membrane formation by oligodendrocytes. Mol Cell Neurosci 1999;14:199–212. [PubMed: 10576890]

Buttery PC, ffrench-Constant C. Process extension and myelin sheet formation in maturing oligodendrocytes. Prog Brain Res 2001;132:115–130. [PubMed: 11544981]

Clair T, Lee HY, Liotta LA, Stracke ML. Autotaxin is an exoenzyme possessing 5′-nucleotide phosphodiesterase/ATP pyrophosphatase and ATPase activities. J Biol Chem 1997;272:996–1001. [PubMed: 8995394]

Clair T, Aoki J, Koh E, Bandle RW, Nam SW, Ptaszynska MM, Mills GB, Schiffmann E, Liotta LA, Stracke ML. Autotaxin hydrolyzes sphingosylphosphorylcholine to produce the regulator of migration, sphingosine-1-phosphate. Cancer Res 2003;63:5446–5453. [PubMed: 14500380]

Cohen RI. Exploring oligodendrocyte guidance: ‘to boldly go where no cell has gone before’. Cell Mol Life Sci 2005;62:505–510. [PubMed: 15747057]

Cohen RI, Rottkamp DM, Maric D, Barker JL, Hudson LD. A role for semaphorins and neuropilins in oligodendrocyte guidance. J Neurochem 2003;85:1262–1278. [PubMed: 12753085]

NIH-PA Author Manuscript

NIH-PA Author Manuscript

NIH-PA Author Manuscript

Dennis J, Nogaroli L, Fuss B. Phosphodiesterase-Ialpha/autotaxin (PD-Ialpha/ATX): a multifunctional protein involved in central nervous system development and disease. J Neurosci Res 2005;82:737–742. [PubMed: 16267828]

Drake SK, Lee KL, Falke JJ. Tuning the equilibrium ion affinity and selectivity of the EF-hand calcium binding motif: substitutions at the gateway position. Biochemistry 1996;35:6697–6705. [PubMed: 8639620]

Dubois-Dalcq M, Behar T, Hudson L, Lazzarini RA. Emergence of three myelin proteins in oligodendrocytes cultured without neurons. J Cell Biol 1986;102:384–392. [PubMed: 2418030]

Dugas JC, Tai YC, Speed TP, Ngai J, Barres BA. Functional genomic analysis of oligodendrocyte differentiation. J Neurosci 2006;26:10967–10983. [PubMed: 17065439]

Ferguson CG, Bigman CS, Richardson RD, van Meeteren LA, Moolenaar WH, Prestwich GD. Fluorogenic phospholipid substrate to detect lysophospholipase D/autotaxin activity. Org Lett 2006;8:2023–2026. [PubMed: 16671772]

Fox MA, Colello RJ, Macklin WB, Fuss B. Phosphodiesterase-Ialpha/autotaxin: a counteradhesive protein expressed by oligodendrocytes during onset of myelination. Mol Cell Neurosci 2003;23:507–519. [PubMed: 12837632]

Fox MA, Alexander JK, Afshari FS, Colello RJ, Fuss B. Phosphodiesterase-I alpha/autotaxin controls cytoskeletal organization and FAK phosphorylation during myelination. Mol Cell Neurosci 2004;27:140–150. [PubMed: 15485770]

Fox MA, Afshari FS, Alexander JK, Colello RJ, Fuss B. Growth cone-like sensorimotor structures are characteristic features of postmigratory, premyelinating oligodendrocytes. Glia 2006;53:563–566. [PubMed: 16355369]

Fuss B, Baba H, Phan T, Tuohy VK, Macklin WB. Phosphodiesterase I, a novel adhesion molecule and/or cytokine involved in oligodendrocyte function. J Neurosci 1997;17:9095–9103. [PubMed: 9364056]

Gard AL, Pfeiffer SE. Oligodendrocyte progenitors isolated directly from developing telencephalon at a specific phenotypic stage: myelinogenic potential in a defined environment. Development 1989;106:119–132. [PubMed: 2697546]

Gijsbers R, Aoki J, Arai H, Bollen M. The hydrolysis of lysophospholipids and nucleotides by autotaxin (NPP2) involves a single catalytic site. FEBS Lett 2003;538:60–64. [PubMed: 12633853]

Guan KL, Dixon JE. Eukaryotic proteins expressed in Escherichia coli: an improved thrombin cleavage and purification procedure of fusion proteins with glutathione S-transferase. Anal Biochem 1991;192:262–267. [PubMed: 1852137]

Hama K, Aoki J, Fukaya M, Kishi Y, Sakai T, Suzuki R, Ohta H, Yamori T, Watanabe M, Chun J, Arai H. Lysophosphatidic acid and autotaxin stimulate cell motility of neoplastic and non-neoplastic cells through LPA1. J Biol Chem 2004;279:17634–17639. [PubMed: 14744855]

Hardy R, Reynolds R. Proliferation and differentiation potential of rat forebrain oligodendroglial progenitors both in vitro and in vivo. Development 1991;111:1061–1080. [PubMed: 1879350]

Hardy RJ, Friedrich VL Jr. Progressive remodeling of the oligodendrocyte process arbor during myelinogenesis. Dev Neurosci 1996;18:243–254. [PubMed: 8911764]

Jiang S, Avraham HK, Park SY, Kim TA, Bu X, Seng S, Avraham S. Process elongation of oligodendrocytes is promoted by the Kelch-related actin-binding protein Mayven. J Neurochem 2005;92:1191–1203. [PubMed: 15715669]

Jockusch BM, Bubeck P, Giehl K, Kroemker M, Moschner J, Rothkegel M, Rudiger M, Schluter K, Stanke G, Winkler J. The molecular architecture of focal adhesions. Annu Rev Cell Dev Biol 1995;11:379–416. [PubMed: 8689563]

Kachar B, Behar T, Dubois-Dalcq M. Cell shape and motility of oligodendrocytes cultured without neurons. Cell Tissue Res 1986;244:27–38. [PubMed: 3516402]

Kilpatrick TJ, Ortuno D, Bucci T, Lai C, Lemke G. Rat oligodendroglia express c-met and focal adhesion kinase, protein tyrosine kinases implicated in regulating epithelial cell motility. Neurosci Lett 2000;279:5–8. [PubMed: 10670774]

Kirby BB, Takada N, Latimer AJ, Shin J, Carney TJ, Kelsh RN, Appel B. In vivo time-lapse imaging shows dynamic oligodendrocyte progenitor behavior during zebrafish development. Nat Neurosci 2006;9:1506–1511. [PubMed: 17099706]

NIH-PA Author Manuscript

NIH-PA Author Manuscript

NIH-PA Author Manuscript

Knapp PE. Injury stimulates outgrowth and motility of oligodendrocytes grown in vitro. Exp Cell Res 1997;234:7–17. [PubMed: 9223365]

Knapp PE, Bartlett WP, Skoff RP. Cultured oligodendrocytes mimic in vivo phenotypic characteristics: cell shape, expression of myelin-specific antigens, and membrane production. Dev Biol 1987;120:356–365. [PubMed: 2435591]

Koh E, Clair T, Woodhouse EC, Schiffmann E, Liotta L, Stracke M. Site-directed mutations in the tumor-associated cytokine, autotaxin, eliminate nucleotide phosphodiesterase, lysophospholipase D, and motogenic activities. Cancer Res 2003;63:2042–2045. [PubMed: 12727817]

Laukaitis CM, Webb DJ, Donais K, Horwitz AF. Differential dynamics of alpha 5 integrin, paxillin, and alpha-actinin during formation and disassembly of adhesions in migrating cells. J Cell Biol 2001;153:1427–1440. [PubMed: 11425873]

Le Clainche L, Plancque G, Amekraz B, Moulin C, Pradines-Lecomte C, Peltier G, Vita C. Engineering new metal specificity in EF-hand peptides. J Biol Inorg Chem 2003;8:334–340. [PubMed: 12589569]

Lee HY, Clair T, Mulvaney PT, Woodhouse EC, Aznavoorian S, Liotta LA, Stracke ML. Stimulation of tumor cell motility linked to phosphodiesterase catalytic site of autotaxin. J Biol Chem 1996;271:24408–24412. [PubMed: 8798697]

Lee J, Jung ID, Nam SW, Clair T, Jeong EM, Hong SY, Han JW, Lee HW, Stracke ML, Lee HY. Enzymatic activation of autotaxin by divalent cations without EF-hand loop region involvement. Biochem Pharmacol 2001;62:219–224. [PubMed: 11389881]

Lewit-Bentley A, Rety S. EF-hand calcium-binding proteins. Curr Opin Struct Biol 2000;10:637–643. [PubMed: 11114499]

Liang X, Draghi NA, Resh MD. Signaling from integrins to Fyn to Rho family GTPases regulates morphologic differentiation of oligodendrocytes. J Neurosci 2004;24:7140–7149. [PubMed: 15306647]

Liu A, Muggironi M, Marin-Husstege M, Casaccia-Bonnefil P. Oligodendrocyte process outgrowth in vitro is modulated by epigenetic regulation of cytoskeletal severing proteins. Glia 2003;44:264–274. [PubMed: 14603467]

Martin KH, Slack JK, Boerner SA, Martin CC, Parsons JT. Integrin connections map: to infinity and beyond. Science 2002;296:1652–1653. [PubMed: 12040184]

Miao H, Burnett E, Kinch M, Simon E, Wang B. Activation of EphA2 kinase suppresses integrin function and causes focal-adhesion-kinase dephosphorylation. Nat Cell Biol 2000;2:62–69. [PubMed: 10655584]

Miller RH. Regulation of oligodendrocyte development in the vertebrate CNS. Prog Neurobiol 2002;67:451–467. [PubMed: 12385864]

Moolenaar WH, van Meeteren LA, Giepmans BN. The ins and outs of lysophosphatidic acid signaling. Bioessays 2004;26:870–881. [PubMed: 15273989]

Murphy-Ullrich JE. The de-adhesive activity of matricellular proteins: is intermediate cell adhesion an adaptive state? J Clin Invest 2001;107:785–790. [PubMed: 11285293]

Murphy-Ullrich JE, Gurusiddappa S, Frazier WA, Hook M. Heparin-binding peptides from thrombospondins 1 and 2 contain focal adhesion-labilizing activity. J Biol Chem 1993;268:26784–26789. [PubMed: 8253815]

Murphy-Ullrich JE, Lane TF, Pallero MA, Sage EH. SPARC mediates focal adhesion disassembly in endothelial cells through a follistatin-like region and the Ca(2+)-binding EF-hand. J Cell Biochem 1995;57:341–350. [PubMed: 7539008]

Narita M, Goji J, Nakamura H, Sano K. Molecular cloning, expression, and localization of a brain-specific phosphodiesterase I/nucleotide pyrophosphatase (PD-I alpha) from rat brain. J Biol Chem 1994;269:28235–28242. [PubMed: 7961762]

Nelson MR, Chazin WJ. Structures of EF-hand Ca(2+)-binding proteins: diversity in the organization, packing and response to Ca2+ binding. Biometals 1998;11:297–318. [PubMed: 10191495]

Nielsen JA, Maric D, Lau P, Barker JL, Hudson LD. Identification of a novel oligodendrocyte cell adhesion protein using gene expression profiling. J Neurosci 2006;26:9881–9891. [PubMed: 17005852]

Olsen IM, ffrench-Constant C. Dynamic regulation of integrin activation by intracellular and extracellular signals controls oligodendrocyte morphology. BMC Biol 2005;3:25. [PubMed: 16283943]

NIH-PA Author Manuscript

NIH-PA Author Manuscript

NIH-PA Author Manuscript

Osterhout DJ, Wolven A, Wolf RM, Resh MD, Chao MV. Morphological differentiation of oligodendrocytes requires activation of Fyn tyrosine kinase. J Cell Biol 1999;145:1209–1218. [PubMed: 10366594]

Peters DM, Herbert K, Biddick B, Peterson JA. Myocilin binding to Hep II domain of fibronectin inhibits cell spreading and incorporation of paxillin into focal adhesions. Exp Cell Res 2005;303:218–228. [PubMed: 15652337]

Pfeiffer SE, Warrington AE, Bansal R. The oligodendrocyte and its many cellular processes. Trends Cell Biol 1993;3:191–197. [PubMed: 14731493]

Prod'hom B, Karplus M. The nature of the ion binding interactions in EF-hand peptide analogs: free energy simulation of Asp to Asn mutations. Protein Eng 1993;6:585–592. [PubMed: 8234229]

Ranjan M, Hudson LD. Regulation of tyrosine phosphorylation and protein tyrosine phosphatases during oligodendrocyte differentiation. Mol Cell Neurosci 1996;7:404–418. [PubMed: 8812065]

Ricard D, Stankoff B, Bagnard D, Aguera M, Rogemond V, Antoine JC, Spassky N, Zalc B, Lubetzki C, Belin MF, Honnorat J. Differential expression of collapsin response mediator proteins (CRMP/ULIP) in subsets of oligodendrocytes in the postnatal rodent brain. Mol Cell Neurosci 2000;16:324–337. [PubMed: 11085871]

Ricard D, Rogemond V, Charrier E, Aguera M, Bagnard D, Belin MF, Thomasset N, Honnorat J. Isolation and expression pattern of human Unc-33-like phosphoprotein 6/collapsin response mediator protein 5 (Ulip6/CRMP5): coexistence with Ulip2/CRMP2 in Sema3a- sensitive oligodendrocytes. J Neurosci 2001;21:7203–7214. [PubMed: 11549731]

Richter-Landsberg C. The oligodendroglia cytoskeleton in health and disease. J Neurosci Res 2000;59:11–18. [PubMed: 10658180]

Savaskan NE, Rocha L, Kotter MR, Baer A, Lubec G, van Meeteren LA, Kishi Y, Aoki J, Moolenaar WH, Nitsch R, Bräuer AU. Autotaxin (NPP-2) in the brain: cell type-specific expression and regulation during development and after neurotrauma. Cell Mol Life Sci 2006;64:230–243. [PubMed: 17192809]

Sloane JA, Vartanian TK. Myosin Va controls oligodendrocyte morphogenesis and myelination. J Neurosci 2007;27:366–11357. [PubMed: 17215397]

Sommer I, Schachner M. Monoclonal antibodies (O1 to O4) to oligodendrocyte cell surfaces: an immunocytological study in the central nervous system. Dev Biol 1981;83:311–327. [PubMed: 6786942]

Song J, Goetz BD, Baas PW, Duncan ID. Cytoskeletal reorganization during the formation of oligodendrocyte processes and branches. Mol Cell Neurosci 2001;17:624–636. [PubMed: 11312599]

Stankoff B, Barron S, Allard J, Barbin G, Noel F, Aigrot MS, Premont J, Sokoloff P, Zalc B, Lubetzki C. Oligodendroglial expression of Edg-2 receptor: developmental analysis and pharmacological responses to lysophosphatidic acid. Mol Cell Neurosci 2002;20:415–428. [PubMed: 12139919]

Tanaka M, Okudaira S, Kishi Y, Ohkawa R, Iseki S, Ota M, Noji S, Yatomi Y, Aoki J, Arai H. Autotaxin stabilizes blood vessels and is required for embryonic vasculature by producing lysophosphatidic acid. J Biol Chem 2006;281:25822–25830. [PubMed: 16829511]

van Meeteren LA, Ruurs P, Stortelers C, Bouwman P, van Rooijen MA, Pradere JP, Pettit TR, Wakelam MJ, Saulnier-Blache JS, Mummery CL, Moolenaar WH, Jonkers J. Autotaxin, a secreted lysophospholipase D, is essential for blood vessel formation during development. Mol Cell Biol 2006;26:5015–5022. [PubMed: 16782887]

Warrington AE, Barbarese E, Pfeiffer SE. Stage specific, (O4+GalC−) isolated oligodendrocyte progenitors produce MBP+ myelin in vivo. Dev Neurosci 1992;14:93–97. [PubMed: 1382941]

Webb DJ, Parsons JT, Horwitz AF. Adhesion assembly, disassembly and turnover in migrating cells -- over and over and over again. Nat Cell Biol 2002;4:E97–100. [PubMed: 11944043]

Weiner JA, Hecht JH, Chun J. Lysophosphatidic acid receptor gene vzg-1/lpA1/edg-2 is expressed by mature oligodendrocytes during myelination in the postnatal murine brain. J Comp Neurol 1998;398:587–598. [PubMed: 9717712]

Williams SK, Spence HJ, Rodgers RR, Ozanne BW, Fitzgerald U, Barnett SC. Role of Mayven, a kelch-related protein in oligodendrocyte process formation. J Neurosci Res 2005;81:622–631. [PubMed: 16035103]

NIH-PA Author Manuscript

NIH-PA Author Manuscript

NIH-PA Author Manuscript

Wilson R, Brophy PJ. Role for the oligodendrocyte cytoskeleton in myelination. J Neurosci Res 1989;22:439–448. [PubMed: 2474666]

Xie Y, Meier KE. Lysophospholipase D and its role in LPA production. Cell Signal 2004;16:975–981. [PubMed: 15212758]

Yu N, Lariosa-Willingham KD, Lin FF, Webb M, Rao TS. Characterization of lysophosphatidic acid and sphingosine-1-phosphate-mediated signal transduction in rat cortical oligodendrocytes. Glia 2004;45:17–27. [PubMed: 14648542]

Zaidel-Bar R, Cohen M, Addadi L, Geiger B. Hierarchical assembly of cell-matrix adhesion complexes. Biochem Soc Trans 2004;32:416–420. [PubMed: 15157150]

Zaidel-Bar R, Milo R, Kam Z, Geiger B. A paxillin tyrosine phosphorylation switch regulates the assembly and form of cell-matrix adhesions. J Cell Sci 2007;120:137–148. [PubMed: 17164291]

Zamir E, Geiger B. Components of cell-matrix adhesions. J Cell Sci 2001;114:3577–3579. [PubMed: 11707509]

Zeller NK, Behar TN, Dubois-Dalcq ME, Lazzarini RA. The timely expression of myelin basic protein gene in cultured rat brain oligodendrocytes is independent of continuous neuronal influences. J Neurosci 1985;5:2955–2962. [PubMed: 2414417]

NIH-PA Author Manuscript
NIH-PA Author Manuscript
NIH-PA Author Manuscript

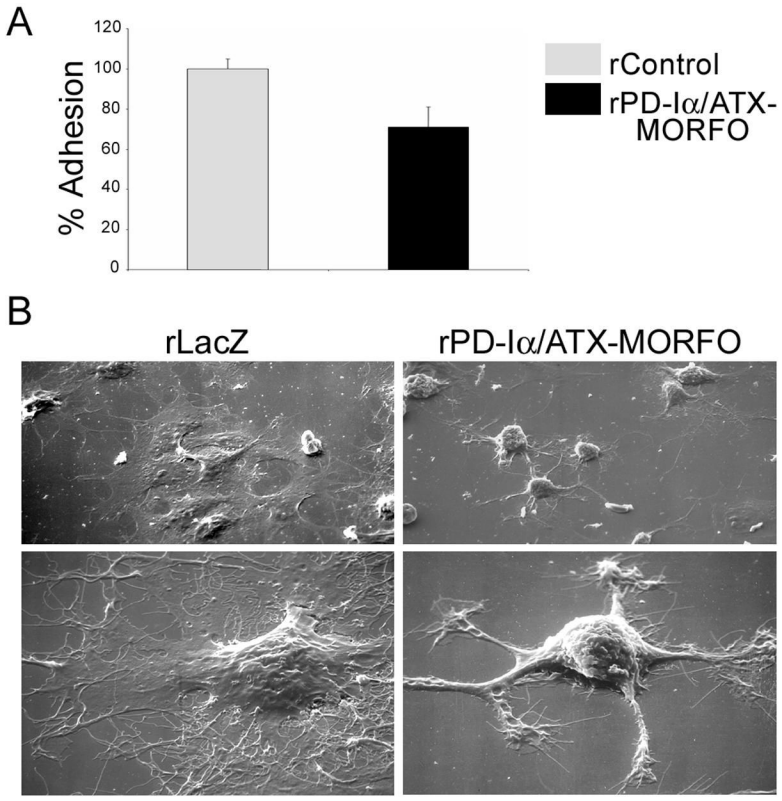

Fig. 1.

PD-Iα/ATX's MORFO domain promotes oligodendroglial process outgrowth. (A) Cells of the immortalized oligodendroglial cell line CIMO were found to be responsive to the adhesion-antagonizing effect of PD-Iα/ATX's MORFO domain. Means and standard errors of three independent experiments done in quadruplicates are shown. Student's *t*-test analysis revealed an overall two-tailed significance level of $p<0.05$. (B) Scanning electron micrographs (SEM) taken at 500x (top panels) and 2000x (bottom panels) magnification and 48° tilt. CIMO cells plated in the presence of rPD-Iα/ATX-MORFO (right panels) extended numerous primary and secondary processes and possessed rounded somas. In contrast, these cells appeared flat and non-process bearing under control conditions (rLacZ; left panels).

NIH-PA Author Manuscript
NIH-PA Author Manuscript
NIH-PA Author Manuscript

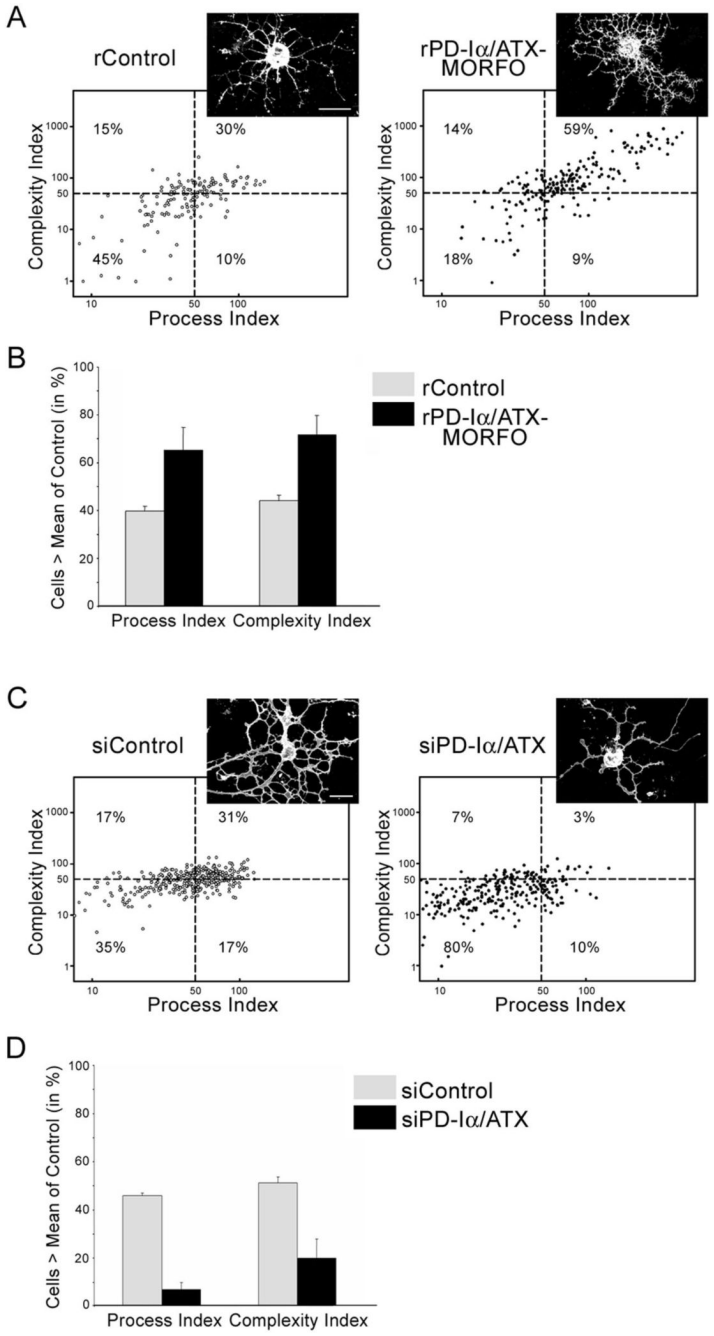

Fig. 2.

PD-Iα/ATX's MORFO domain promotes the extension of a complex process network by post-migratory, premyelinating oligodendrocytes. (A) and (B) Oligodendrocyte progenitor cells were isolated from brains of 3 day-old rats. Cells were plated onto mixed (FN plus rControl (rControl) or FN plus rPD-Iα/ATX (rPD-Iα/ATX)) substrates and after 24 hrs soluble rControl or rPD-Iα/ATX protein was added. 48 hrs after plating cells were immunostained with the O4 antibody to visualize post-migratory, premyelinating oligodendrocytes. (A) Normalized values of the cells' process indices (total amount of O4-positive process surface per cell) were plotted against normalized values of their complexity indices (ratio of process index and network area) on logarithmic scales (mean control value = 50; see dashed lines). Five independent

NIH-PA Author Manuscript

NIH-PA Author Manuscript

NIH-PA Author Manuscript

experiments with at least 30 cells per condition are shown. In the upper right corner of each of the scatter plots a representative confocal image of an O4-positive oligodendrocyte, cultured under the indicated conditions, is depicted. Confocal images represent 2D maximum projections of stacks of 0.5 μm optical sections. Scale Bar: 20 μm. (B) Bar graph illustrating the percentage of cells with a process or complexity index greater than the calculated control mean (means and standard errors are shown). For both parameters, Student's *t*-test analysis revealed an overall two-tailed significance level of $p<0.05$. (C) and (D) O4-positive oligodendrocytes were isolated from brains of 4 day-old rats. Cells were cultured for 48 hrs and treated with a control (siControl) or PD-Iα/ATX-specific (siPD-Iα/ATX) siRNA SMARTpool. 48 hrs after siRNA transfection cells were immunostained with the O4 antibody and analyzed as in (A) and (B). Means and standard errors are shown in B. For both parameters, Student's *t*-test analysis revealed an overall two-tailed significance level of $p<0.05$. Scale Bar: 20 μm.

NIH-PA Author Manuscript
NIH-PA Author Manuscript
NIH-PA Author Manuscript

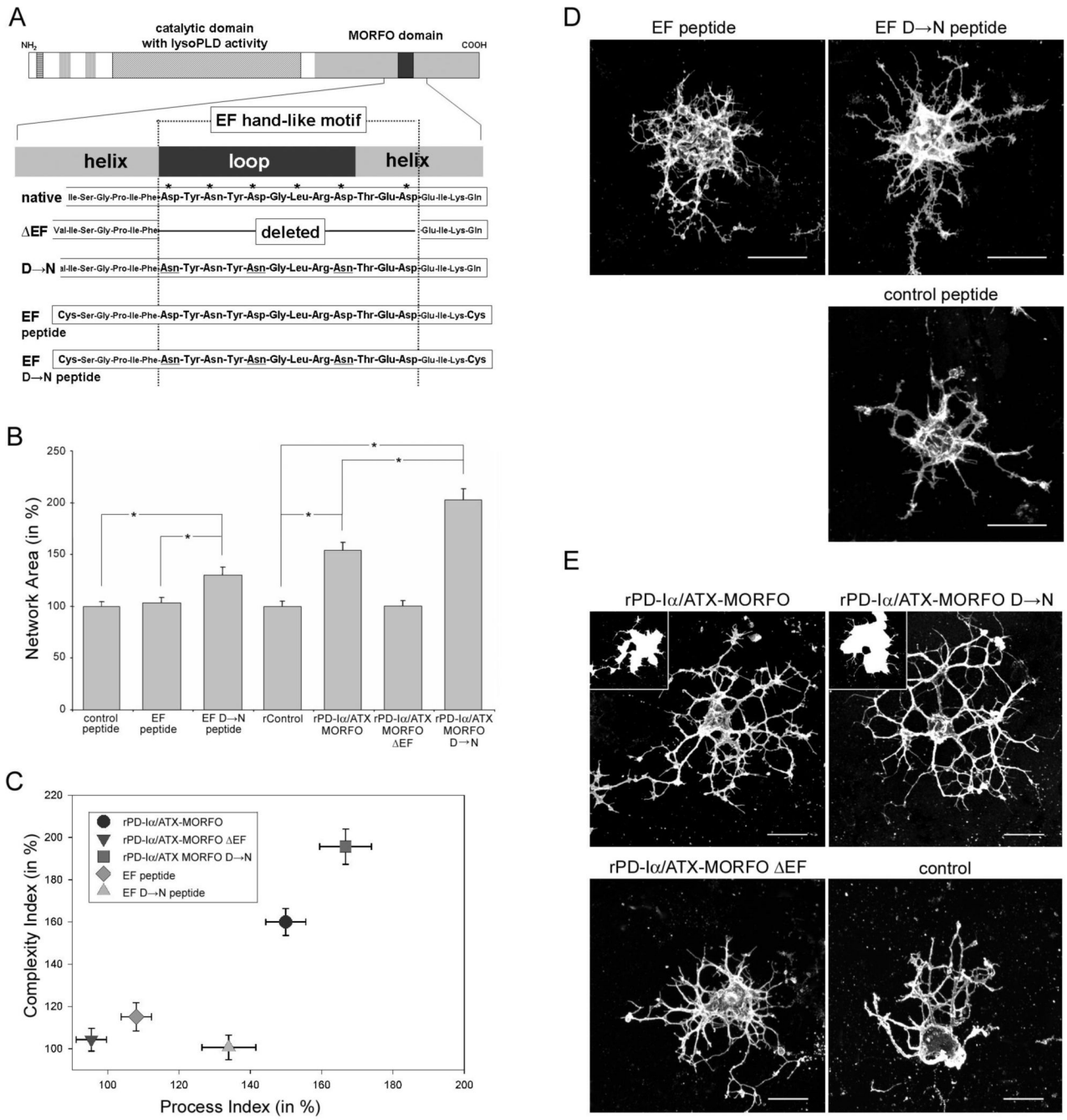

Fig. 3.

PD-Iα/ATX's MORFO domain promotes oligodendroglial process network formation in part via its EF hand-like motif. (A) Structure-function domains of full length PD-Iα/ATX (top) and detailed sequence information for the region around the EF hand-like motif (bottom). The MORFO domain and the loop region of the EF hand-like motif are indicated by a light and dark gray box, respectively. PD-Iα/ATX's catalytic domain is represented by a diagonally striped box, its two somatomedinB domains by vertically striped boxes and the signal peptide crucial for secretion by a horizontally striped box. Protein sequences are noted for native and mutated (ΔEF and D→N) recombinant (r)PD-Iα/ATX-MORFO fusion proteins and for the peptides representing PD-Iα/ATX's EF hand loop region in its native (EF peptide) and mutated

NIH-PA Author Manuscript

NIH-PA Author Manuscript

NIH-PA Author Manuscript

(EF D→N peptide) form. Mutated amino acid residues are underlined. Conserved amino acid residues characteristic for EF hand loops are indicated by an asterisk above the native sequence. (B) Bar graph representing the areas occupied by the cells' process networks (network area = white area in insets to E, upper panel). Mean control network areas were set to 100% and experimental network area values adjusted accordingly. In the bar graph, means and standard errors are shown. Stars indicate overall two-tailed significance levels of $p<0.05$ (Student's *t*-test). (C) 2D graph representing process index (X-axis) and complexity index (Y-axis) of all cells in the presence of native or mutated (ΔEF and D→N) recombinant (r)PD-Iα/ATX-MORFO fusion proteins, as well as native (EF peptide) or mutated (EF D→N peptide) peptides. Control indices were set to 100% and experimental index values adjusted accordingly. In the graph, means and standard errors are shown. (D) and (E) Representative examples of oligodendrocytes cultured in the presence of control, EF or EF D→N peptide (D) and rPD-Iα/ATX-MORFO, rPD-Iα/ATX-MORFO D→N, rPD-Iα/ATX-MORFO ΔEF or control protein (E). Cells were isolated and treated as in the experiments to Fig. 2A and B. Confocal images represent 2D maximum projections of stacks of 0.5 μm optical sections. Scale Bar: 20 μm (note that the magnification is higher in D than in E).

NIH-PA Author Manuscript
NIH-PA Author Manuscript
NIH-PA Author Manuscript

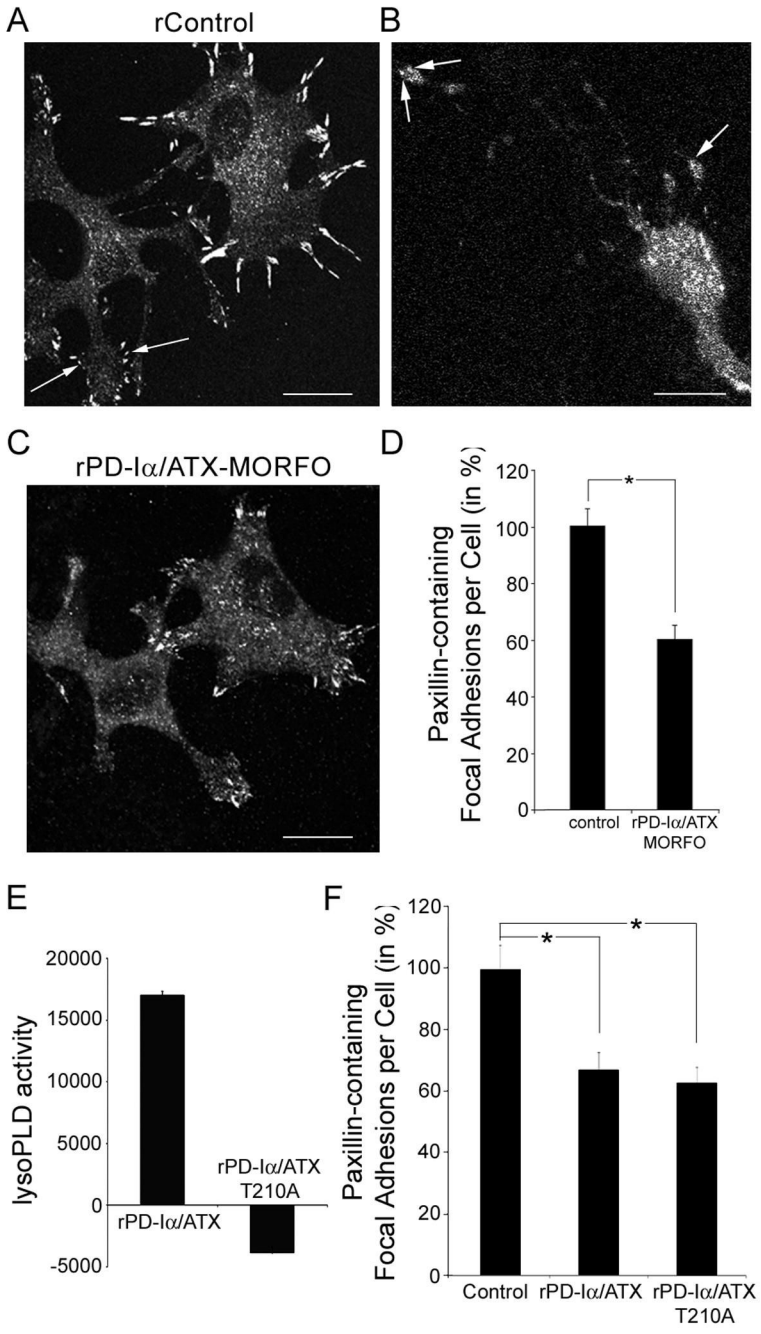

Fig 4.

Paxillin-containing focal adhesions are present at the leading edge of oligodendroglial protrusions and their number is diminished in the presence of PD-Iα/ATX's MORFO domain. (A) CIMO cells were plated in the presence of rControl protein for 1 hr. Under these conditions focal adhesions located toward the leading edge of cellular protrusions were detectable by immunocytochemical staining for paxillin. (B) Similar to CIMO cells paxillin-containing focal adhesions (see arrows) were detected in OLG-growth cones of primary oligodendrocytes nucleofected with a plasmid encoding paxillin-EGFP. (C) CIMO cells were plated in the presence of rPD-Iα/ATX-MORFO for 1 hr and immunostained for paxillin. Compared to control conditions (A) a decrease in the number of paxillin-containing focal adhesions was

NIH-PA Author Manuscript

NIH-PA Author Manuscript

NIH-PA Author Manuscript

noticed. (D) Quantification of focal adhesions after immunostaining of CIMO cells plated on the different substrates. Bar graph depicts the number of paxillin-containing focal adhesions per cell as % of control (mean of control = 100%). (E) Quantification of PD-Iα/ATX's lysoPLD activity. Full length rPD-Iα/ATX, native (rPD-Iα/ATX) and mutated (rPD-Iα/ATX-T210A), was purified from stably transfected Cos-7 cells and lysoPLD activity was determined using the fluorogenic assay described by Ferguson et al. (2006). A typical example done in triplicates is depicted in the graph. Numbers on the Y-axis represent fluorescent intensities. (F) CIMO cells were plated onto fibronectin-coated glass coverslips in the presence of 0.1 μg/ml control (Control), native rPD-Iα/ATX (rPD-Iα/ATX) or enzymatically inactive rPD-Iα/ATX (rPD-Iα/ATX-T210A) protein. Paxillin-containing focal adhesions per cell were determined as in D. In all bar graphs, means and standard errors are shown. Stars indicate an overall two-tailed significance level of $p<0.05$ (Student's *t*-test). Arrows in (A) indicate smallest sized focal adhesions counted (approximately 1 μm^2) for the bar graphs in (D) and (F). Confocal images in (A), (B) and (C) represent optical sections approximately 250 nm in depth and close to the basal surface. Scale Bars: 20 μm in (A) and (C); 10 μm in (B).

NIH-PA Author Manuscript
NIH-PA Author Manuscript
NIH-PA Author Manuscript

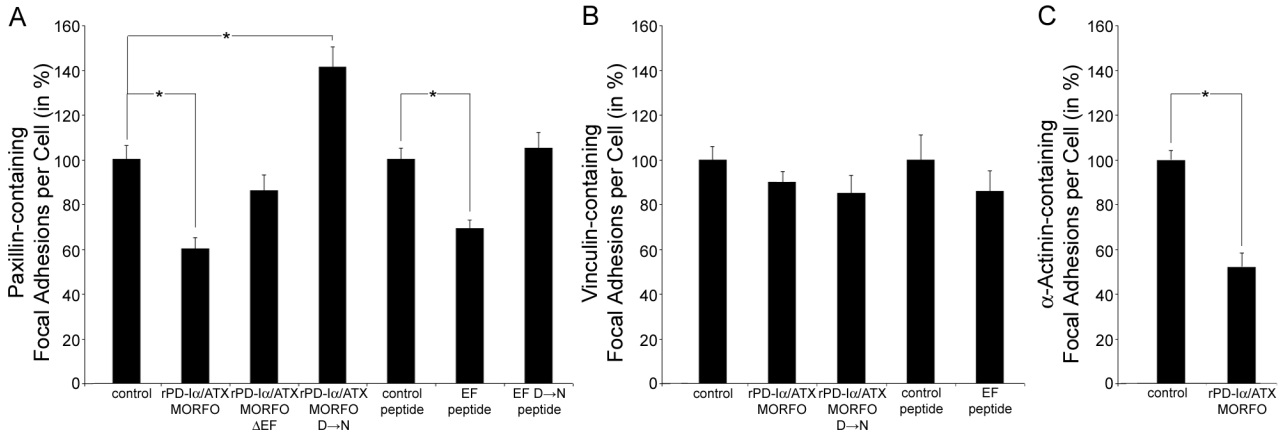

Fig. 5.

PD-Iα/ATX's MORFO domain mediates a reduction in the number of detectable paxillin-containing focal adhesions via its EF hand-like motif. In addition, PD-Iα/ATX's MORFO domain reduces the number of detectable α-actinin- but not vinculin-containing focal adhesions. (A–C) CIMO cells were plated for 1 hr in the presence of fusion protein or peptide (see label below each bar and Fig. 3A) and cells were immunolabeled for paxillin (A), vinculin (B) or α-actinin (C). The graphs illustrate the percentage of paxillin-, vinculin- or α-actinin-containing focal adhesions per cell as % of control (mean of control = 100%). Means and standard errors are shown. The stars indicate overall two-tailed significance levels of $p<0.05$ (Student's *t*-test).

NIH-PA Author Manuscript
NIH-PA Author Manuscript
NIH-PA Author Manuscript

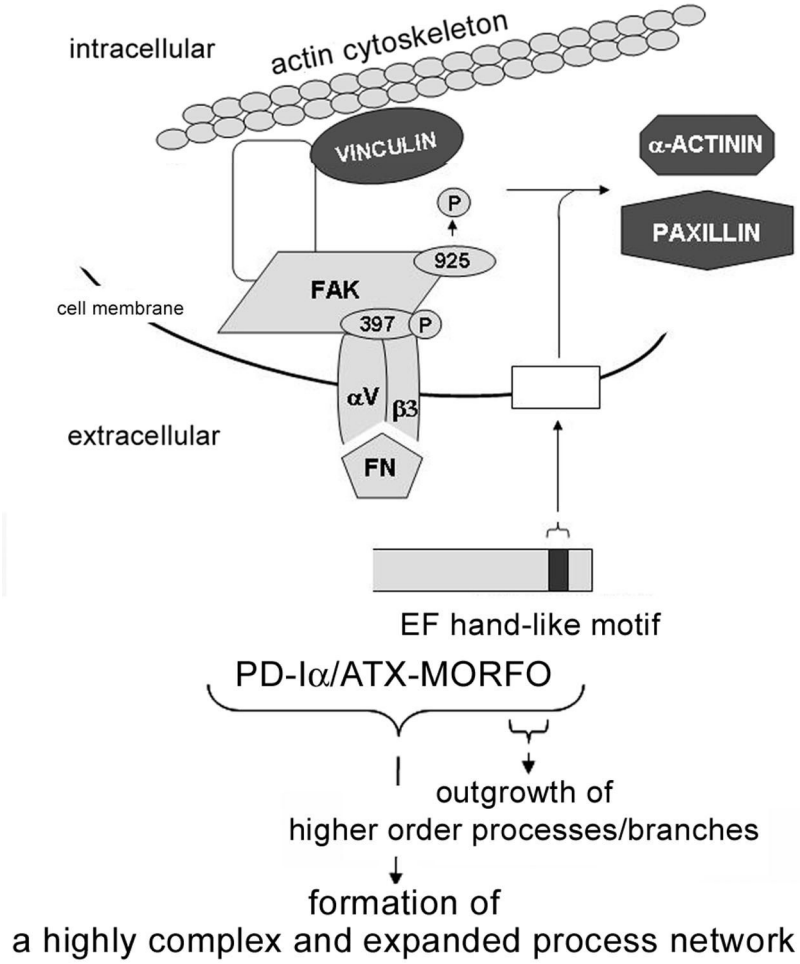

Figure 6.

Proposed model of the functional properties of PD-Iα/ATX's MORFO domain toward post-migratory, premyelinating oligodendrocytes. As described previously (Fox et al., 2004), PD-Iα/ATX's MORFO domain induces adhesion-antagonism (symbolized by the distance between the integrin receptor (α and β) and the ECM constituent fibronectin (FN)) through a mechanism likely involving a yet to be identified cell surface receptor (white rectangle). In addition, the MORFO domain causes dephosphorylation at the tyrosine residue 925 (925) of focal adhesion kinase (FAK) without significantly affecting the phosphorylation of the tyrosine residue 397 (397P). Thus, FAK appears to remain associated with an integrin-containing complex at the cell surface. The data presented here further demonstrate that PD-Iα/ATX's MORFO domain, likely via its EF hand-like motif, promotes a loss of paxillin and α-actinin from focal adhesions, thereby weakening the link between the ECM and the cytoskeleton and promoting the outgrowth of in particular higher order processes/branches. Vinculin distribution appears largely unaffected, suggesting that similar to FAK it remains associated with a protein complex located at the cell surface. Vinculin is not known to directly bind to either FAK or integrins. Thus, it is likely bound to the cell surface-associated complex via a yet to be identified adaptor protein (white rectangle with rounded edges). PD-Iα/ATX's MORFO domain as a whole promotes not only the outgrowth of higher order processes but also stimulates process elongation and thus the formation of a highly complex and expanded process network.